Chapter in **Advancing Astrophysics with the SKA – II**

Dual AGN and Multiple SMBH Systems in the Era of SKAO

Quirino D'Amato,[1*] Lang Cui,[2] Roger Deane,[3] S. Komossa,[4] Coral Pillay,[3] Ashutosh Tripathi,[2] Preeti Kharb,[5] Hengxiao Guo,[6] Sumana Nandi,[7] Khatun Rubinur,[8] Sonia Anton,[9] Tao An,[6] Silvia Bonoli,[10] Ning Chang,[2] Romeel Dave,[11] Alessandra De Rosa,[12] Melanie Habouzit,[13] Filippo Mannucci,[1] Isabella Prandoni,[14] Paola Severgnini,[15] Martina Scialpi,[16] Cristiana Spingola,[14] Cristian Vignali,[17] Wancheng Xu,[2] Xi Yan[2] and Yingkang Zhang[6]

[1]*INAF – Osservatorio Astrofisico di Arcetri, Via Largo E. Fermi 5, Firenze 50125, Italy*

[2]*Xinjiang Astronomical Observatory, CAS, 150 Science-1 Street, Urumqi 830011, China*

[3]*Wits Centre for Astrophysics, University of the Witwatersrand, 1 Jan Smuts Avenue, Johannesburg, 2000, South Africa*

[4]*Max-Planck-Institut für Radioastronomie, Auf dem Hügel 69, 53121 Bonn, Germany*

[5]*National Centre for Radio Astrophysics (NCRA) - Tata Institute of Fundamental Research (TIFR), S. P. Pune University Campus, Ganeshkhind, Pune 411007, India*

[6]*Shanghai Astronomical Observatory, CAS, 80 Nandan Road, Shanghai, China*

[7]*Institute of Astronomy Space and Earth Sciences, P 177, CIT Road, Scheme 7m, Kolkata 700054, West Bengal, India*

[8]*Institute of Theoretical Astrophysics, University of Oslo, P.O. Box 1029, Blindern, 0315 Oslo, Norway*

[9]*CFisUC, Departamento de Física, Universidade de Coimbra, 3004-516 Coimbra, Portugal*

[10]*Donostia International Physics Center (DIPC), Paseo Manuel de Lardizabal 4, 20018 Donostia-San Sebastian, Spain & IKERBASQUE, Basque Foundation for Science, E-48013, Bilbao, Spain*

[11]*Institute for Astronomy, Royal Observatory, University of Edinburgh, Edinburgh EH9 3HJ, UK*

[12]*INAF - Istituto di Astrofisica e Planetologia Spaziali, Via del Fosso del Cavaliere I-00133, Roma, Italy*

[13]*Department of Astronomy, University of Geneva, Chemin d'Ecogia, CH-1290 Versoix, Switzerland*

[14]*INAF - Istituto di Radioastronomia, Via P. Gobetti 101, I–40129, Italy*

[15]*INAF - Osservatorio Astronomico di Brera, via Brera 28, I-20121 Milano, Italy & via Bianchi 46, Merate (LC), Italy*

[16]*Dipartimento di Fisica e Astronomia, Università di Firenze, via G. Sansone 1, 50019 Sesto F.no, Firenze, Italy*

[17]*Dipartimento di Fisica e Astronomia, Università degli Studi di Bologna, Via P. Gobetti 93/2, 40129, Bologna, Italy*

[*]*Corresponding author: Email: quirino.damato@inaf.it*

We present a radio-oriented review of current strategies for the detection and characterization of dual active galactic nuclei (DAGN) and supermassive black holes binaries (SMBHBs), emphasizing the crucial role of radio interferometry in advancing this field. We discuss how high-resolution radio imaging – particularly through very long baseline interferometry (VLBI) – provides an unique, dust-unbiased tool to identify multiple accreting SMBHs, disentangle AGN-related emission from star formation, and trace components from tens of kpc to sub-parsec scales. We summarize current observational limitations, such as insufficient sensitivity–resolution combination and area coverage. We then outline how the SKAO will overcome these constraints through its unprecedented combination of sensitivity, survey speed, imaging fidelity and angular resolution, enabling the discovery and characterization of dual and binary SMBHs from the nearby Universe to the epoch of reionization. Several science cases are presented, including radio follow-ups of optical/infrared-selected DAGN, direct blind radio selection of DAGN, studies of compact bound SMBHBs, and the link between SMBHB orbital evolution and low-frequency gravitational wave emission. We further emphasize the synergy between SKAO observations and modern and upcoming facilities such as the James Webb and Euclid space telescopes, Rubin observatory, and gravitational wave detectors including the laser interferometer space antenna and pulsar timing arrays. These combined capabilities will allow SKAO to enable the first comprehensive radio census of dual and binary SMBH systems, bridge the gap between electromagnetic and gravitational wave observations, and provide a statistically significant view of SMBH pairing, accretion, and merger-driven feedback throughout cosmic history.

1 Introduction

Super-massive black holes (SMBHs), with masses of $\sim 10^6 - 10^9$ $M_\odot$, are believed to reside ubiquitously in galactic centers, particularly in the bulge of elliptical and spiral galaxies (see Kormendy and Richstone, 1995; De Rosa et al., 2019, and references therein). The tight observational correlations between SMBHs masses and properties of their host galaxies, such as stellar velocity dispersion, strongly suggest a fundamental co-evolution between SMBHs and their galactic environments over cosmic timescales (Kormendy and Ho, 2013). A primary mechanism driving both galaxy and SMBH growth is hierarchical merging: hydrodynamical simulations show that galaxy major mergers produce gas inflows towards the center of galaxies, which can trigger both star formation (SF) and accretion onto their central SMBHs, producing luminous active galactic nuclei (AGN, Di Matteo et al., 2005; Mayer et al., 2007). As a result of the inspiraling merging process, multi-SMBH systems form (Begelman et al., 1980; Volonteri et al., 2003). In particular, dual AGN (DAGN) are systems where two active SMBHs have a separation larger than their radii of gravitational influence, but still evolving within the potential of the merged host galaxies (Merritt, 2013; Volonteri et al., 2022). These objects, typically found at hundreds of pc up to tens of kpc separation, are considered the direct precursors of SMBH binaries (SMBHBs), where two SMBHs are gravitationally bound, usually at pc to sub-pc scales ($\lesssim$10 pc, Mayer et al., 2007; Dotti et al., 2007).

The study of these multi-SMBH systems is of paramount importance for several reasons. They offer crucial insights into the intricate interplay between galaxy mergers and SMBHs fueling and growth, enabling tests of the many predictions of galaxy evolution models. Examples of testable predictions are their separation distribution, their number density, fraction in the overall AGN population, redshift evolution, the mass and luminosity ratios between the primary and secondary components, the impact on host galaxies, and many others (Volonteri et al., 2022; Shen et al., 2023; Di Matteo et al., 2023). Moreover, SMBHBs are predicted to be the primary sources of low-frequency (nHz-μHz) gravitational waves (GWs) in the Universe (Jaffe and Backer, 2003; Sesana, 2013; Colpi et al., 2019), making them key targets for GW observatories such as the laser interferometer space antenna (LISA, Amaro-Seoane et al. 2023) and pulsar timing arrays (PTAs, Agazie et al., 2023; EPTA Collaboration et al., 2023).

Observationally, however, directly detecting and characterizing these systems, especially at small separations and high redshifts, remains a significant challenge due to their inherent rarity, and the large sky area coverage and resolution required to select and confirm a significant amount of candidates (De Rosa et al. 2019; see also Sec. 1.1 and Sec. 1.2). Radio emission is an unique tool to identify multiple SMBHs candidates and confirm their nature; it is not affected by dust obscuration (Deane et al., 2014), it can be observed down to sub-arcsecond resolution thanks to the interferometry technique (milli-arcsecond for very long baseline interferometry, VLBI) and it is not affected by spurious emission of gas photo-ionization region "mimicking" a second AGN like in optical data (Fu et al., 2012). However, current cm-wavelength surveys with sub-arcsec resolution are limited by either shallow sensitivity and/or small area coverage. The advent of next-generation facilities, particularly the Square Kilometre Array Observatory (SKAO), promises to revolutionize this field by providing an unparalleled ability to discover, characterize, and study multi-SMBH

systems across a vast range of cosmic distance and orbital separation, thanks to the unmatched sensitivity, survey speed and imaging fidelity, combined with the high angular resolution that it will achieve.

1.1 The quest of finding high-z DAGN

Given the large galaxy merger timescale (~1 Gyr, Tremmel et al., 2017), the presence of DAGN is expected for $\gtrsim$ 1% of bright ($L_{\rm bol} > 10^{43}$ erg s^{-1}) AGN at $z \gtrsim 2$ (Volonteri et al., 2003, 2022). While many dual systems at $z > 0.5$ are needed to robustly test model predictions, identifying these systems is a difficult task because it requires large sky area coverage with sub-arcsec resolution (De Rosa et al., 2019). X-ray emission has been used in the past to select these systems, but due to low photon-counting statistics and coarse resolution in wide area surveys, the detection/characterization of candidates is practically possible only in the nearby Universe (De Rosa et al., 2019). Currently, the most promising selection techniques rely on the optical emission of relatively bright quasars ($G_{\rm mag} \lesssim 21$; Shen et al., 2019; Mannucci et al., 2022). In the last few years, techniques based on the precise astrometry and the high resolution offered by the *Gaia* all-sky survey (Gaia Collaboration et al., 2024) emerged as efficient methods to select high-z DAGN. In particular, the "varstrometry" and *Gaia*-multi-peak (GMP) selection criteria allowed to discover tens of new dual systems at $z > 0.5$ down to few kpc projected separation. The "varstrometry" technique selects DAGN candidates on the basis of the extra-astrometric noise produced by luminosity variability of the members of an otherwise unresolved dual system (Shen et al., 2019). The GMP method, instead, searches for multiple peaks in the light profiles of optically/infrared-selected quasars in the *Gaia* archive (Mannucci et al., 2022); this technique led to the selection of hundreds of DAGN candidates with sub-arcsecond separation, between 0.15" and ~0.7" (e.g. Mannucci et al., 2023; Ciurlo et al., 2023; Scialpi et al., 2024). A complete census of confirmed DAGN at $z > 0.5$ and projected separation <30 kpc is shown in Fig. 1.

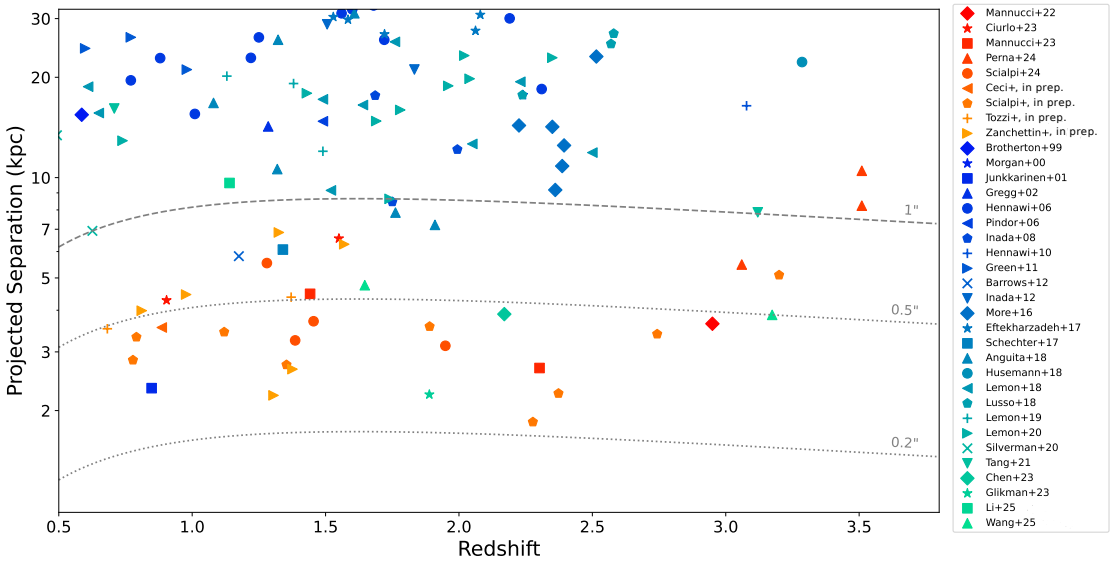

Figure 1: Projected separations of all spectroscopically confirmed high-z DAGN, identified at projected separation $\leq$ 30 kpc and in the $0.5 \leq z \leq 3.5$ range. Updated from Mannucci et al. (2023).

Despite the promises offered by these novel techniques, time-expensive spectroscopy of each target is still required to confirm multiple SMBHs systems, since optically selected objects could be in general associated to DAGN, gravitationally-lensed systems (GLS), or a projected alignment between an AGN and a foreground star. In this context, follow-up observations in the radio band have increasingly become a standard method for uncovering the nature of optically selected systems. Radio compact cores detected in correspondence of the optical/infrared centroids are an effective method to strengthen the DAGN nature of the candidates (Glikman et al., 2023). Radio observations are also useful for excluding GLS contaminants by comparing the optical morphology and multi-band flux ratios of the components (see Sec. 2). In addition, cross-matching *Gaia* and radio VLBI astrometry has proven beneficial for studying quasar jet systems (e.g. Makarov et al., 2017; Plavin et al., 2019; Petrov et al., 2019) and for identifying binary AGN (Breiding et al., 2021). Candidate binary AGN can also be identified via radio-optical positional offsets (Skipper and Browne, 2018).

The selection of DAGN candidates directly in the radio band has the potential to add hundreds of new DAGN candidates, and to uncover the hidden (and mostly unknown) population of obscured DAGN (Deane et al., 2014). Modern interferometers can reach $\sim \mu$Jy/beam sensitivity and cover large sky areas with modest time investment with respect to other wavelengths. Radio AGN are traditionally classified as radio-loud (RL) or radio-quiet (RQ) based on the ratio between their radio and optical (or X-ray) emission (Terashima and Wilson, 2003); the RQ AGN usually overcome the RL population at $\lesssim$ 100 μJy (Bonzini et al., 2013). Thanks to the sensitivity of the new radio surveys, also this faint RQ population, traditionally missed by previous generation, shallower wide-field surveys, has started to be detected and studied (D'Amato et al., 2022; Hale et al., 2025). Furthermore, the James Webb space telescope (JWST) is currently expanding the high-z frontier, including important discoveries of high-z AGN and highest-redshift galaxy pairs and mergers (Duan et al., 2025; Perna et al., 2025). As many of the mergers in the high redshift universe are highly obscured, sensitive radio observations provide an additional or alternative route of finding AGN in these systems. However, the origin of radio emission is unclear: when the $\sim$ 100 μJy regime is approached, it could be ascribed to both AGN or SF activity. In this regime, the radio-excess criterion (i.e., the radio emission in excess with respect to that expected from SF) is commonly adopted to select AGN, yielding a fraction of radio-excess sources of approximately 30% (Smolčić et al., 2017).

While VLBI provides the milli-arcsecond resolution necessary to resolve compact DAGN, it remains technically constrained for broad demographic studies. Current VLBI observations are primarily limited to bright sources (>1 mJy at 1.4 GHz), and up to 70% of the radio flux can be resolved out when larger-scale structures, such as jets, are present (Spingola et al., 2020). Furthermore, the narrow, arcsecond-scale field of view (FOV) of current VLBI arrays makes them unsuitable for blind surveys. As a result, the radio properties of faint, high-z DAGN have not yet been explored in statistically significant, homogeneous samples (e.g., Fu et al., 2012; Deane et al., 2014; Spingola et al., 2019; Glikman et al., 2023; Xu et al., 2024; Schwartzman et al., 2025). Nevertheless, in some low-redshift DAGN with sub-kpc separations, VLBI remains an effective tool for identifying multiple BHs (see Sec. 1.2).

An effective way to distinguish between AGN and SF radio emission is to measure the equivalent

brightness temperature T_b (Condon et al., 1980). AGN typically exhibit $T_b \gtrsim 10^5$ K at 1.4 GHz, with the threshold primarily set by observing frequency (Condon et al., 1980; Morabito et al., 2022). While milli-arcsecond resolution is required at GHz frequencies, the higher threshold at 144 MHz ($T_b \sim 10^6$ K) allows AGN identification at sub-arcsecond resolution scales. This method has enabled the efficient selection of hundreds of radio AGN in LOFAR/LoTSS using international baselines (Shimwell et al., 2017; Morabito et al., 2022).

1.2 Local DAGN and compact bound binary SMBHs

1.2.1 Local DAGN at the centers of single galaxies, still spatially resolved

A number of wide-separation SMBH pairs located at the centers of *single* galaxies or very advanced mergers have been identified in the nearby universe using hard X-ray or radio observations (e.g., Komossa et al., 2003; Deane et al., 2014; Rubinur et al., 2019). These systems are challenging to identify at optical wavelengths because the vast majority of gas-rich mergers are heavily obscured by large columns of dusty gas (Sanders and Mirabel, 1996).

The hard X-ray (up to 10 keV) imaging spectroscopy capabilities of *Chandra* have been particularly successful in detecting even heavily obscured pairs in the local Universe (De Rosa et al., 2019). However, *Chandra* lacks the required sensitivity to systematically assess the AGN pair fraction among the broader population of luminous and ultra-luminous, gas-rich mergers, since sufficiently sensitive spectra cannot be obtained within moderate exposure times (Iwasawa et al., 2011). In addition, angular resolution constraints also limit the X-ray study of these systems: at $z = 0.1$ *Chandra* can only resolve scales down to approximately 1.8 kpc.

Recent high-resolution, multi-wavelength studies have revealed several benchmark DAGN systems on sub-kiloparsec to parsec scales, offering key insights into the late stages of galaxy and BH co-evolution. In NGC 6240, a luminous infrared galaxy (LIRG) at $z = 0.024$ in an advanced merger, *Chandra* imaging first confirmed two obscured, hard X-ray nuclei separated by ~750 pc, each showing Fe Kα emission (Komossa et al., 2003). Later optical spectroscopy suggested a possible third nucleus (Kollatschny et al., 2020). UGC 4211, with a ~230 pc separation, was identified as a dust-obscured AGN by the wide-field infrared survey explorer (WISE) and confirmed by the Hubble space telescope (HST), Keck telescope, and Atacama large millimeter/submillimeter array (ALMA) imaging (Koss et al., 2023). Similarly, MCG–03–34–64 hosts a ~100 pc dual AGN revealed by Fe Kα emission, where complementary HST and very large array (VLA) radio imaging provided crucial confirmation of both active nuclei (Trindade Falcão et al., 2024), underscoring the vital role of radio observations in penetrating obscured regions and distinguishing compact AGN cores in merging systems. The identification of sub-kpc separation DAGN candidates can also be effectively carried out through multi-epoch VLBI observations, such as in the case of J1543-0757 (~130 pc; Cheng and Sohn, 2024).

Local LIRGs and ultra-LIRG (ULIRGs) are especially suited candidates to identify DAGN in the nearby Universe, as they trace merging galaxies at different stages of the merging sequence. In this respect, radio observations are of paramount importance in isolating true BH accretion activity from contaminants (such as starburst, see Sec. 1.1). The exceptional sensitivity and angular resolution of SKAO will allow one to carry a complete radio census of LIRGs and ULIRGs along

merger sequences (early-to-late merger), allowing to bridge the gap between high-z DAGN and local SMBHBs.

1.2.2 Compact and radio-detected SMBHBs

Compact, gravitationally bound SMBHs that have reached or surpassed the so-called "final parsec" of orbital evolution (Begelman et al., 1980; Merritt, 2013), represent the final stage of the BH merging sequence. Despite their expected abundance (Volonteri et al., 2022), no unambiguous sub-parsec binary SMBH has yet been confirmed, largely due to the extreme angular resolution and sensitivity required to directly resolve such compact systems. Even with the state-of-the-art VLBI facilities, most searches rely on indirect signatures or are limited by the radio faintness of one component.

One of the most widely adopted strategies for identifying sub-pc SMBHBs is detecting AGN with (quasi-)periodic variations in their photometric light curves (Tripathi et al., 2024). This periodicity arises from accretion disk interactions, orbital Doppler boosting and, in the radio-band, jet precession. Among periodic light-curve candidates, OJ 287 remains the canonical example. Its ∼12 yr double-peaked optical outbursts had in the past been interpreted by a variety of different models including jet precession, jet beaming due to orbital motion, or accretion-disk impact models (e.g., Sillanpaa et al., 1988; Valtonen et al., 2008; Katz, 1997; Villata et al., 1998; Valtaoja et al., 2000). Recent results have shown that the latest outburst of OJ 287 is dominated by non-thermal emission as predicted by jet-related outburst models (Komossa et al., 2023a,b), and a similar conclusion was reached for several previous outbursts (Gopal-Krishna, 2024). Similarly, as example, PG 1302-102 and PKS 2131-021 have shown quasi-periodic variability in the optical and radio bands, respectively (Graham et al., 2015; O'Neill et al., 2022). However, in general, distinguishing genuine periodic signals from stochastic variability (red noise) intrinsic to a single AGN remains a challenge. Recent multi-wavelength and radio spectro-photometric analyses have demonstrated that binary models for OJ 287 require a low primary mass and disk luminosity, calling for revised modeling in a new parameter regime (Komossa et al., 2023a,b). Currently, in order to rule out stochastic or noise-driven fluctuations, long time multi-band observations are required to confirm true periodicity (Vaughan et al., 2016; El-Badry et al., 2025). Furthermore, SMBHBs may be detected via radio-transient phenomena, either due to temporary switch off of jet activity between the rapid SMBHBs shrinking phase and the post-coalescence new accretion disk formation (Milosavljević and Phinney, 2005), or due to stellar tidal disruption event (TDE, Liu et al. 2014, Shu et al. 2026). Another promising approach – enabled by radio VLBI position accuracy – is tracing the sub-pc scale orbital motion induced by the spiraling BHs, using the radio technique of phase referencing. The 3C 66B source, one of the most studied SMBHB candidates, was initially identified with this technique, by precisely measuring the elliptical periodic offset of the (multi-band) radio-emission centroid in a Keplerian period of ∼1 yr, on scales of few hundreds of μas (Sudou et al., 2003). The advantage of this technique is that only one of the two BHs (preferentially the less massive) has to be radio-active.

Alternative search methods in the radio band relies on the large-scale structure morphology, such as the jets and lobes (Spingola et al., 2026). One is the search for helical or precessing radio jets, whose morphology may arise from orbital motion or from torque-induced jet precession in a binary system (Conway and Wrobel, 1995). Despite the difficulty in distinguishing such signatures from

magnetic-field-driven helices, this technique has been applied in a few cases, such as NGC 1275 (Liu and Chen, 2007). Another technique relies on the detection of multiple episodes of jet activity, marked by multiple pairs of radio-lobes (double-double radio galaxies, DDRGs). In most DDRGs, outer lobes with steeper spectra trace past AGN activity, while inner lobes mark renewed outbursts. A rare subset, the "misaligned DDRGs", shows jet reorientation likely caused by torques from a secondary SMBH in a non-coplanar orbit (Nandi et al., 2017). VLBI monitoring reveals evolving pc-scale structures and variable radio cores (Nandi et al., 2024). Signatures of a multiple BHs system can be also unveiled by the well-known S-, Z-, and X-shaped radio galaxies. In these systems, jet precession or reorientation – driven by a secondary SMBH or disk realignment – produces symmetric radio lobes. Such morphologies fit jet-precession models implying sub-parsec separations and are further supported by double-peaked optical emission lines (e.g., Rubinur et al., 2017; Kharb et al., 2019; Misra et al., 2025).

Finally, radio-VLBI observations currently represent the only method able to resolve the pc-scale separated SMBHBs population. As an example, the radio galaxy 0402+379 remains the most compact SMBHB candidate imaged to date. Multi-frequency very long baseline array (VLBA) observations resolved two flat-spectrum, variable radio cores separated by only 7.3 pc (Rodriguez et al., 2006), and subsequent multi-epoch VLBI astrometry over 12 years detected relative motion between them (Bansal et al., 2017). Pc-scale and sub-pc-scale binaries have been suggested in other AGN (e.g., Deane et al., 2014; Kharb et al., 2017); these require further observations and monitoring.

1.2.3 Linking to multi-messenger astronomy

Upon final coalescence, bound binary SMBHs are the loudest sources of gravitational waves in the Universe (e.g. Colpi et al., 2024); the lower-mass coalescences (chirp masses below $\sim 10^7$ $M_\odot$) will fall in the sensitivity regime of future space-based GW interferometers like LISA, while the highest-mass coalescences (chirp masses above 10^8 $M_\odot$) are in the regime of PTAs. The recent detection of a GW background signal is consistent with a population of SMBHBs mergers (e.g., Agazie et al., 2023; Mingarelli et al., 2025). These results are already helping constraining models for the assembly of SMBHs (Toubiana et al., 2024; Bonoli et al., 2025). Radio observations play an invaluable role in future multi-messenger astrophysics of merging BHs. Coalescing SMBHBs would appear as radio transients (see above), once the inner disk and jet disappears shortly before coalescence, and then re-forms afterwards, and with the GW signal from coalescence in-between. Depending on the timescales and detections, any dipping radio source could represent an alert of an upcoming GW event, or an observed GW event could motivate a search for a later radio transient signal. While electromagnetic transients can also be identified in other wavebands, the radio SKAO regime is unique in combining high sensitivity and high spatial resolution, and is thus also invaluable in pinpointing the location of the counterpart (see Sec. 5). In addition, as aforementioned, jetted TDEs that occur in evolved binary SMBH systems have characteristically different lightcurves than jetted TDEs around single SMBHs (Donnarumma et al., 2015). High-sensitivity radio observations are essential in order to follow the lightcurve evolution and model the binary orbit. As long as Swift-type X-ray transient missions operate, this approach can also be followed in X-rays (whenever the centers are not heavily absorbed), but it comes with a degeneracy

that is sometimes difficult to overcome, given that both the accretion disk and jet emit strong X-ray emission, while the radio emission uniquely points to the presence of jets. This fact provides a major advantage when modeling these systems. In general, radio observations are fundamental to isolated transients signatures (such as jet precession and tidal disruption) involving the presence of SMBHBs at advanced merging stages, complementary to GW detectors. As an example, radio monitoring in combination with multi-wavelength observations of OJ 287 have also demonstrated that this system is in the LISA sensitivity regime upon coalescence (Komossa and Grupe, 2024). Another example is the aforementioned case of 3C 66B: while the binary nature of the source has been identified with radio phase reference technique, a significant part of the parameter space of orbital solutions could already be excluded based on PTA constraints (Jenet et al., 2005). In ongoing/upcoming transient surveys at other wavelengths, such as in the optical with the Rubin large synoptic survey telescope (LSST), or in X-rays with Swift, the discovery of exceptionally large numbers of new, unidentified transients is expected (Ivezić et al., 2019). Follow-up spectroscopic observations of all of these are prohibitively time consuming. Sensitive radio observations will immediately allow us to distinguish between different source types in a way that is more challenging (or not possible) with optical and X-ray observations alone.

1.3 Bridging the gap with simulations

Understanding the prevalence and evolution of DAGN is central to linking galaxy mergers with BH growth. Cosmological hydrodynamic simulations and semi-analytical models of galaxy formation and evolution provide a powerful framework for exploring this connection, but they remain limited by fundamental trade-offs: large volumes are required to capture rare DAGN systems, while high resolution is needed to follow the small-scale physics of BH dynamics, accretion, and feedback. Achieving both] is computationally expensive, and only a few recent simulations are able to resolve AGN pairs on kpc scales (De Rosa et al., 2019).

DAGN, a key phase in the hierarchical assembly of galaxies, are especially sensitive to the complex interplay of subgrid processes that shape BH and galaxy dynamics both before and after the host galaxy mergers. As a result, variations in model assumptions lead to discrepancies of several orders of magnitude in the predicted number counts (Puerto-Sánchez et al., 2025). These discrepancies could arise from a combination of many factors, including different selection functions, initial BH masses, BH accretion efficiency and stellar/AGN feedback prescriptions among the several simulations. Some simulations also find that the AGN feedback is so effective that it prevents the formation of DAGN in the most massive galaxies (Puerto-Sánchez et al., 2025; Habouzit et al., 2022). On the one hand, the distribution of projected separations would constrain the dynamical evolution of BH pairs, revealing the physical processes that govern inward migration, the first phase of which is dynamical friction. On the other hand, the redshift distribution of DAGN will provide a direct link between the timing of BH growth and the assembly of cosmic structures.

2 SKAO Science Case 1: Confirmation of high-z DAGN candidates

The robust identification and characterization of DAGN at small ($<$ 1 arcsec) angular separation remains one of the major observational challenges in extragalactic astrophysics. Although

promising progress has been made in the optical domain and a growing population of DAGN candidates has identified, the unambiguous confirmation of such systems requires complementary multi-wavelength observations (see Sec. 1.1). In particular, since the ultimate confirmation requires spatially-resolved spectroscopy – only available through time-expensive observations either from ground (with adaptive optics) or space observatories – it is necessary to preliminary refine the selection only to observe the strongest candidates. This process is currently carried mainly through ground-based unresolved spectroscopy, aiming at removing the AGN-star contaminant systems that feature clear star absorption lines in the primary AGN spectra (Scialpi et al., 2024). However, depending on the separation, component flux ratio, spectra quality and galactic latitude, the efficiency of this method significantly varies from case to case. In addition, these methods can not reveal the second most important contaminant in DAGN selection, that are GLS. In this context, radio follow-ups can serve as a powerful tool to efficiently refine the selection of DAGN, helping in isolating only the strongest candidates; radio compact cores detected in correspondence of the optical centroids are an effective method to identify the DAGN nature of the candidates (Glikman et al., 2023). In addition, if multi-frequency observations are available, radio data can be used to measure the spectral index of the AGN synchrotron emission, further restricting the selection to flat-spectrum cores, although steep spectrum nuclei have also been detected especially in low luminosity AGN (Giroletti and Panessa, 2009; Panessa and Giroletti, 2013; Kharb et al., 2021). As for the GLS contamination, we note that strong lensing is independent from the observed frequency, thus the flux ratio of the multiple images of a lensed source are expected to be the same in different bands. Then, if resolved imaging data (much time-cheaper than spectroscopy) at other bands are available, they can be coupled with radio images to exclude the lensing contaminants by comparing the flux ratio in different bands. Furthermore, multi-epoch radio observations can also be used to unveil the nature of multiple radio images: by pinpointing the radio cores and, potentially, measuring their motion over time to track their orbits (e.g., Spingola et al. 2019), the radio band offers the most definitive method for confirming the dual nature of such systems.

As discussed in Sec 1.1, the application of VLBI to DAGN has historically been limited by flux loss and FOV constraints. By studying radio-detected $\lesssim$1 mJy DAGN at $z \lesssim 0.2$ with $\lesssim$3 arcsec separation, Xu et al. (2024) showed that 75% of single AGN are undetected with VLBI, indicating that most pc-scale emission is resolved out. Although this effect is reduced at higher redshift, VLBI still probes only tens of parsecs at $0.5 < z < 3$, potentially missing larger-scale structures such as jets. With SKAO, the synergy between optical and radio astronomy will be fully realized. Current optical-based methods can select DAGN at <1 arcsec resolution down to Gaia magnitude $M_G = 20.5-21$ (see Sec 1.1). This means that, given the radio flux limitation imposed by VLBI with current facilities, the majority of dual systems hosting RQ AGN are ruled out from the analysis, and their characteristics are not explored yet. SKA-Mid can easily overcome these limitations. Based on the Anticipated Performance[1] and SKAO sensitivity calculator (SSC[2]) predictions, the most suited band for our purpose – starting from AA* – configuration, will be Band 5a (4.6 – 8.5 GHz). The dense *uv*-coverage offered by SKA-Mid antennas will offer a stable sensitivity in a wide range of scales (0.35" - 21" at 6.5 GHz in configuration AA*), ensuring the full recovering

[1] https://www.skao.int/en/science-users/122/relevant-documents
[2] https://sensitivity-calculator.skao.int/

of the source total flux. At the targeted redshift range ($0.5 \lesssim z \lesssim 3$), 0.35" corresponds to ~ 2.1 - 2.7 projected kpc, allowing to disentangle the DAGN components without resolving out the sub-kpc emission of each AGN. The resolution offered by AA* in Band 5a falls in this maximum sensitivity "sweet spot" range, making possible to efficiently separate the components at an angular distance comparable to that reached by current optical selection method. This will allow for the first time to investigate the RQ counterparts of optically-selected DAGN. As example, we assume a nominal target flux density of 100 μJy at 1.4 GHz, traditionally considered the flux density at which the extragalactic radio sky starts to be dominated by RQ AGN (D'Amato et al., 2022, and reference therein). Conservatively assuming a spectral index $\alpha = -0.7$ (radio core are expected to be "flat-spectrum" sources), describing the synchrotron flux density at frequency ν ad $S_\nu \propto \nu^\alpha$, we derive an expected ~35 μJy at 6.5 GHz. Assuming a conservative 50% fractional bandwidth, with the SSC we estimate that just in 10 min observation such an emission can be observed at $\sim 7\sigma$ significance down to a resolution of 0.3", using a visibility weighting suited to balance resolution and sensitivity (Briggs robustness = 0). With an uniform weighting SKA-Mid AA* will reach 0.15" – 0.05" resolution, allowing to disentangle components beyond the current optical-selection capabilities. The downgrade in sensitivity can be easily overcome: ~2 h observations can reach the same $\sim 7\sigma$ detection significance. Once AA4 will be operative, it will extend the stable sensitivity in the 0.15" - 21" range of scales, fully unlocking the SKAO potential in optically-selected DAGN follow-ups.

The synergy between optical observatories and SKAO will not only offer an efficient way to strengthen the DAGN selection, but it will also allow to investigate their physics and interaction with the external environment. It is now well-established that the radio loudness is connected with BH accretion efficiency (Merloni et al., 2003). For single AGN, it is observed that those hosted by early-type galaxies show lower efficiency than in gas-rich systems, both in the local Universe (Panessa et al., 2015) and at high redshifts (D'Amato et al., 2022). With a representative sample of optical-selected DAGN detected at radio frequencies we could compare the accretion efficiencies in these systems with those of single AGN. The SKAO sensitivity will allow for the first time to efficiently sample DAGN in the RQ regime (i.e. the vast majority of the population) and in the distant Universe, and put stringent constraints to the radio-detected fraction of optical emitters as a function, for example, of physical separation. Whether the brightest optical component in a DAGN also corresponds to the brightest radio emitter is not straightforward, as the two bands typically probe different accretion regimes. Hydrodynamical simulations, moreover, predict that a large fraction of the most massive BH may reside in the faintest component of the DAGN (Chen et al., 2023); SKAO observations can test these predictions in the radio band down to the nJy regime, ultimately tracing differences with the optical emission of both components.

As for the very high redshift population, the detection of DAGN way beyond the cosmic noon ($z > 3$, Mannucci et al., 2022; Yue et al., 2023; Perna et al., 2025), and even up to the cosmic dawn ($z \gtrsim 6$, Yue et al., 2021; Matsuoka et al., 2024; Übler et al., 2024), has started to be increasingly reported in recent years. In general, the number of radio-detected AGN at $z \gtrsim 6$ is a small fraction of the known systems, while the vast majority (~75%) is classified as RQ on the basis of upper limits (Bañados et al., 2015). While SKAO will in general revolutionize the study of radio AGN population at the cosmic dawn, it will also enable the identification of radio counterparts of confirmed DAGN.

The faintest $z \gtrsim 6$ AGN 3σ radio upper limits are of the order of $\sim 20\mu$Jy at 1.4 GHz (Bañados et al., 2015), corresponding to $\sim 5\mu$Jy at 6.5 GHz if $\alpha = -0.7$. As example, in just ~50 h of AA* observations the entire population of currently known DAGN at $z > 3.5$ can be observed down to a 3σ sensitivity of $\sim 0.75\mu$Jy/beam with enough resolution to disentangle their components, immediately opening a new window on the characterization of these objects.

Finally, we note that most of ongoing ground-based surveys searching for DAGN are carried out with adaptive optics instruments (e.g., MUSE, ERIS) mounted on 8-m class telescopes in the Southern Hemisphere (Mannucci et al., 2022, 2023; Scialpi et al., 2024). As a result, most of the identified candidates are not observable with the major radio facilities located in the Northern Hemisphere, such as VLA, VLBA, and LOFAR-VLBI. SKAO will allow for the first time to efficiently complement these ongoing and future surveys, both in confirming candidates and studying the radio properties of confirmed objects.

3 SKAO Science Case 2: Radio selection of high-z DAGN

The selection of DAGN in the radio band has been inefficient to date due to technical limitations of current facilities in terms of sensitivity vs. resolution combination. As an example, the deepest available VLA surveys reach few μJy/beam noise level at 1.4 GHz, with at maximum ~1.5" resolution (see D'Amato et al., 2022, and reference therein). Higher frequencies are ruled out due to the small FOV and intrinsic fainter emission. As a result, the radio-selected population of high-z DAGN is currently unknown. Investigating their properties will be crucial not only to unveil the hidden obscured fraction of DAGN, but also to test many theoretical predictions. Coupled with optical follow-ups (necessary to confirm the DAGN candidate nature), the radio luminosity can be used to investigate, for example, the radio-optical displacements, radio-loudness, the relation with the BH mass and Eddington ratio ($f_{\rm Edd}$) and the accretion efficiency. A comprehensive census of the radio DAGN population will allow to discern between different evolutionary scenarios, with particular regard to the AGN feedback mode and the origin of the radio emission (Volonteri et al., 2003, 2022; Tremmel et al., 2017; Chen et al., 2023; Shen et al., 2023). Current radio luminosities and fluxes of DAGN are predicted on the basis of many different prescriptions. For example, they can be driven by the BH masses in numerical simulations and *assumed* accretion efficiency and merger delay, and subsequently derived from the fundamental plane (Merloni et al., 2003; Gültekin et al., 2009; Volonteri et al., 2022); otherwise, they can be inferred from the total radio power by making assumption on the accretion model efficiency and kinetic energy conversion in theoretical models (Meier, 2001). All these different recipes and assumptions yield several dex of uncertainty in the expected radio fluxes and in the number of DAGN that will be detected by SKAO (Dong-Páez et al., 2023).

Given the aforementioned premises, we adopt as a reference the latest hydrodynamical simulation predictions presented by Puerto-Sánchez et al. (2025). In their work the number density of DAGN (nDAGN) as a function of redshift are presented for a number of hydrodynamical simulation (including Illustris, TNG50, TNG100, TNG300, EAGLE, SIMBA, Astrid, Horizon AGN; see reference therein), for different thresholds of intrinsic bolometric luminosity $L_{\rm bol}$ and host-galaxy

stellar mass M_*. In particular, we are interested in the nDAGN of the faintest threshold adopted $L_{\rm bol} > 10^{43}$ erg/s, for the less massive host galaxies ($M_* = 10^9$ M$_\odot$). As aforementioned, to date there are no theoretical prescription to derive the radio luminosity $L_{\rm rad}$ from the total luminosity, and current conversions rely on empirical relations. The most studied radio correlation, both at low and high redshift, is with the X-ray emission, that is well-established for orders of magnitude of BH masses and AGN luminosities (Merloni et al., 2003; Panessa et al., 2015; D'Amato et al., 2022). Thus, firstly we converted the luminosity limit $L_{\rm bol} = 10^{43}$ erg/s to X-ray luminosity, adopting for consistency the same theoretical relation reported by Puerto-Sánchez et al. 2025 (see their Eq. 3; see also Shen et al. 2020). Then, we converted the X-ray luminosity to $L_{\rm rad}$ at 1.4 GHz adopting the relation reported by D'Amato et al. (2022). This relation has been derived from the so-called "J1030" field, that features one of the deepest joint X-ray and radio extragalactic survey to date, and is valid for RQ AGN in the $0 \lesssim z \lesssim 3$ redshift range. We note that whether these relations hold for DAGN is currently unknown, especially for the closest pairs hosted by the same galaxy. However, a study of local radio-selected DAGN showed that their X-ray properties are similar to those of single AGN (Gross et al., 2019). The luminosity has been finally converted to the observed $S_{1.4\ \rm GHz}$ at 1.4 GHz, assuming $\alpha = -0.7$. In Fig. 2 we report the number of DAGN per deg^2 as a function of redshift, predicted by the several aforementioned simulations. The solid red line represents $S_{1.4\ \rm GHz}$ for a $L_{\rm bol} = 10^{43}$ erg/s source.

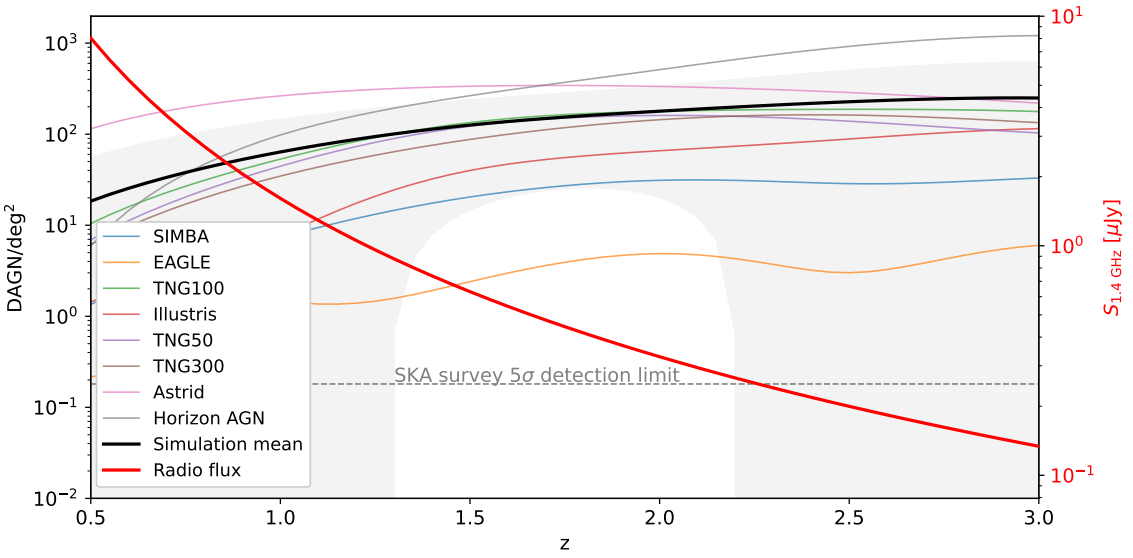

Figure 2: Number of DAGN per deg^2 as a function of redshift, for a number of hydrodynamical simulations. The thick black solid line is the mean of the simulations, while the gray area is the standard deviation. The thick red solid is the expected flux density at 1.4 GHz for a $L_{\rm bol} = 10^{43}$ erg/s AGN. The grey dashed horizontal line is the 5σ detection threshold for the deep reference survey of $\sim$ 1 deg^2 at 1.4 GHz proposed by Prandoni and Seymour (2015).

In Prandoni and Seymour (2015) a reference deep SKAO survey of $\sim$ 1 deg^2 at 1.4 GHz was proposed, aiming at reaching rms$\sim$50 nJy/beam with a resolution of $\sim$0.5". With current AA4 specifications, the survey can be carried out in $\sim$1000 h. While its main scientific driver is investigating the SF and BH accretion history of the Universe, such a survey will be also of great

benefit in efficiently selecting radio high-z DAGN for the first time. As shown in Fig. 2, DAGN where both the components have $L_{\rm bol} > 10^{43}$ erg/s can be detected up to $z \sim 2.2$ and down to 3-4 kpc projected separation. As a reference, current optically-based selection method can only detect DAGN with $L_{\rm bol} > 10^{45}$ erg/s: SKAO will completely revolutionize the field, allowing for the first time to study both the faint and obscured DAGN populations. Importantly, it will lead to the detection of potentially hundreds of new DAGN systems at the epoch of the cosmic noon ($z \sim 2$), that is where both the SF and BH accretion histories peak. For brighter sources ($L_{\rm bol} > 10^{44}$ erg/s), the search can be extended up to $z \sim 4$. We also stress that predictions reported by Puerto-Sánchez et al. (2025) refer to BHs still seating in 2 distinct galaxies; thus, their predicted nDAGN can be considered lower limits.

The selection and confirmation of DAGN in the radio band has to be complemented by ancillary data. A reference survey like that proposed by Prandoni and Seymour (2015) will be likely followed-up by multi-wavelength photometric observations, like usually did for other deep radio surveys (e.g., Smolčić et al., 2017; D'Amato et al., 2022). This will, for example, enable the measurement of photometric redshifts and start formation rates of the optical counterparts, thereby allowing contaminants to be removed (Delvecchio et al., 2017). As mentioned in Sec. 1.1, the μJy radio sky at GHz frequencies is dominated by star-forming galaxies (SFG), thus complementary information from optical/infrared bands are needed to isolate the AGN emission. In addition, a maximum separation of 30 kpc would correspond to 5" – 4" angular separation in the $0.5 < z < 3$ range; while spurious source pairs closer than this on the sky plane represent only a small fraction in current deep μJy high-resolution surveys (e.g., 5% – 3% in J1030), the increasing of source spatial density in the nJy regime can lead to a significant fraction of spurious association, if only radio separation criterion is used. Moreover, many radio sources can appear as a pair of point-like emission if only the hot-spots of the jets are detected. On the other hand, as shown by the multiwavelength characterization of the 3 GHz COSMOS survey (Smolčić et al., 2017), the radio band is crucial to unveil many low-to-moderated luminosity AGN, that are often missed by photometric classification: in a considerable fraction (16%) of sources classified as SFG, the presence of the AGN could only be determined by the detection of the so-called "radio-excess[3]". In addition, AGN-powered radio-emission is often detected also in sources that are optically-classified as simple quiescent galaxies (Smolčić et al., 2017; D'Amato et al., 2022).

Finally, we want to stress that, as mentioned in Sec. 1.1, the most reliable way to confirm radio AGN emission without relying on multiwavelength follow-ups is through the measurement of the brightness temperature at low frequencies (~150 MHz), if sub-arcsecond angular resolution is achieved (Morabito et al., 2022). Low-frequency observations have also benefits in detecting steep-spectrum emission and better isolate point-like AGN cores. In this respect, SKA-Low would in principle represent an huge step forward for studies of distant single and dual AGN. However, the lack of baselines longer than ~80 km for SKA-Low will allow for a maximum resolution of only ~10", insufficient to resolve sub-arcsecond DAGN. A future SKA-Low upgrade, providing at least a factor of ~ 4 longer baselines, is necessary to fill the gap with LOFAR, which is the major current

[3] Radio luminosity that is significantly higher than that expected from SF only, as inferred from standard infrared-radio relations.

SKAO pathfinders at these frequencies, and that will implement automated acquisition and data-reduction of international baselines in the ongoing 2.0 upgrade. This upgrade would be particularly important considering that SKA-Low will be the only next-generation low-frequency instrument to have access to the entire Southern Sky, unlocking the full potential of the synergy with current and future Southern optical/infrared facilities. The lack of long baselines, however, can be mitigated by the development of a low-frequency VLBI network incorporating the SKA-Low (Kobayashi et al., 2026).

4 SKAO Science Case 3: SMBHBs evolution, from wide-separation to the merger

SKAO radio observations play a fundamental role in searching for wide AGN pairs in the populations of galaxy mergers. As mentioned in Sec. 1.2, a complete radio census of LIRGs and ULIRGs along the merger sequences would be a great application. These galaxies are characterized by dust-enshrouded accretion processes and, due to their merging galaxy nature, are optimal candidates to harbor merging BHs at intermediate stages between kpc-scale separated DAGN (still residing in different host galaxies) and $\lesssim$ 1 pc SMBHBs. The inner radio-band emission can pierce the dense inter-stellar medium, and such observations can help in characterizing the physics of the merging BHs and interaction with their host galaxies. Accretion onto SMBHs occurs through both radiatively efficient and inefficient processes. Each of these modes drives distinct feedback mechanisms that shape the host galaxy's evolution, and can be found in both RQ and RL AGN. Which is the impact –if any – of the presence of two active BHs in shaping the properties of the final host galaxy is currently unknown (recent resolved ALMA observations of $0.4 < z < 0.8$ dual AGN suggest an increased gas fraction with respect to single AGN; Tang et al. 2025). SKAO will expand evolutionary studies to include the sub-μJy RQ AGN population, while also being sensitive to the onset and earliest stages of RL AGN activity in the Universe. If intrinsic radio emission is present on pc-scales (i.e., single AGN emission is not resolved down to mas resolutions – see caveats in Sec. 1) such as in NGC 6240 (Sec. 1.2), SKA-VLBI will be able to detect *and* separate single Seyfert nuclei in similar sources up to a factor of, e.g., $\times$15 in distance (for a 5σ detection, assuming the faintest NGC 6240 radio component at 1.7 GHz and 10 hour SKA-Mid Band 2 observation). SKAO exceptional sensitivity and wide survey coverage will also enable detections reaching back to the epoch of the first AGN formation (z> 7; Prandoni and Seymour 2015). Joint with the exceptional sensitivity of JWST in the infrared band, SKAO will be able to investigate the earliest ULIRGs population, helping in isolating the SF from AGN activity. As example, REBELS-25 at $z = 7.3$ is one of the highest redshift ULIRG detected by JWST (Hygate et al., 2023). With a infrared luminosity of $L_{\rm IR} \sim 1.5 \times 10^{12}$ L$_\odot$ erg/s, and assuming that only 20% of it can be ascribed to the AGN, the source would be detected at 1.4 GHz up to $z \sim 8$ in future reference surveys (see Sec. 3 and Prandoni and Seymour 2015). Even if the single BH binaries could not be resolved, the SKAO-JWST synergy will extend the study of RQ/RL AGN towards the epoch of re-ionization; this will allow to investigate if, on a statistical base, merging ULIRGs have different BH-accretion properties with respect to single-galaxy AGN hosts.

Another paramount advancement that SKA-VLBI will bring, particularly important to unresolved $\lesssim$ 1 pc SMBHBs science, is the exceptional astrometry accuracy that will offer (Paragi et al., 2015).

As mentioned in Sec. 1.2, phase reference technique has been successfully applied to measure the Keplerian period of the inspiralling BHs in 3C 66B. High astrometry precision is needed to trace the orbit on this scales, with a orbit major axis of ~ 250 μas at 2.3 GHz and only ~ 50 μas at 8.3 GHz (i.e., sensible to the inner jet emission). While modern VLBI interferometers can reach sufficient precision to carry out these observations, SKA-VLBI is expected to increase by an order of magnitude the astrometry precision (Li et al., 2024). This will allow to trace the smallest orbital periods in the local Universe, or sources such as 3C 66B at much higher redshift. The exceptional astrometric accuracy of SKA-VLBI will also be a fundamental tool in combination with the upcoming *Gaia* Data Release 4 (DR4), which will offer multi-epoch astrometric measurement, and thus enabling a new technique to be used to select SMBHBs. In the radio, compact synchrotron cores trace the vicinity of accreting SMBHs, whereas optical/near-IR light is dominated by the stellar component and provides a proxy for the host's stellar-barycentric photocenter. Significant radio-optical centroid offsets are therefore expected in bound SMBH pairs with dissimilar accretion states or in post-merger recoils (Skipper and Browne, 2018). Pinpointing such centroid offsets is challenging, requiring exquisitely precise, well-calibrated astrometry and a stable radio–optical frame tie. The SKA-Mid AA* phase will pioneer astrometric searches for binary and off-center SMBHs, offering sufficient sensitivity and resolution for targeted pilot studies. It will establish selection thresholds, quantify systematics (core shift, jet contamination, lensing), and demonstrate mas-level differential astrometry on bright, compact sources. At 5 GHz, AA* provides ~0.3" beams, corresponding to ~0.6–2.6 kpc over $z = 0.1 - 4$. In AA*+VLBI mode, phased SKA-Mid can form four simultaneous VLBI beams within its primary field, enabling true in-field multi-view calibration. This suppresses atmospheric and geometric errors, achieving sub-mas relative astrometry and allowing sub-kpc displacement tests, with tens-of-parsec resolution over $z \approx 0.5-2$. The SKA-Mid AA4 phase will deliver ~80 mas beams at 5 GHz, directly resolving ~0.15–0.6 kpc over $z = 0.1 - 4$. In AA4+VLBI, Earth-scale baselines yield mas–sub-mas resolution and $\lesssim$mas differential astrometry, reaching tens of μas for bright, compact cores (1 mas ~ 6–7 pc at $z = 0.5-4$). Combined with Euclid and Rubin/LSST host and variability data, and *Gaia* DR4 epoch astrometry, these will enable the first statistically robust sample and demographic constraints on binary and recoiling SMBHs in the pc–kpc regime. However, we note that at centimeter wavelengths the central engine may be physically offset from the radio core, by up to $10^3 - 10^5$ gravitational radii along the jet (Lobanov, 1998; Marscher et al., 2008). This potential displacement must be accounted for when interpreting radio-optical centroid offsets in candidate binary systems.

The analysis of transient phenomena will be fundamental to investigate the physics of the final stages of SMBHBs merges, i.e. the sources of GW that will be detected by LISA and PTAs (see Sec. 1.2). The SKAO will detect the progenitors of the merging BHs (with $\sim 10^4 - 10^7$ $M_\odot$) that LISA will later characterize. Together, these two observatories will provide a comprehensive view of the full evolutionary pathway from galaxy mergers to BH coalescence, as well as the physical mechanisms driving BH accretion throughout galaxy mergers. Furthermore, the population of the most massive SMBHBs ($M_{\rm BH} \gtrsim 10^9$ $M_\odot$) will be directly constrained with increasing precision using the SKA-Mid and PTAs (Shannon et al., 2026; Takahashi et al., 2026).
Both jetted TDE and disk accretion disruption (and post-coalescence re-formation) events are expected to happen temporarily close to the merging event, and they would produce a significant

variation in the observed radio flux. In the LISA frequency and sensibility range, GW source can be started to be detected days or months before the coalescence, depending on the BHs mass and redshift. As example, a SMBHBs with total mass of 10^6 $M_\odot$ at $z = 3$ will be detected by LISA approximately 1 month before merging (Sesana, 2021). However, also depending on the SMBHBs mass and redshift, the astrometric uncertainty of the event can be up to several hundreds and square deg, reducing to a few square deg ∼1 day before merging (e.g., Mangiagli et al., 2020). In this frame, SKAO will be of great value in identify the upcoming GW counterpart (Anderson et al., 2026). As example, a proposed wide-area reference survey will cover all the observable sky (∼31000 deg^2) at 1.4 GHz, down to 5 μJy/beam sensitivity. When a GW event starts to be detected by LISA, a monitoring of the corresponding area can be triggered with SKAO. Thanks to the unique combination of sensitivity and large FOV (1 deg^2 at 1.4 GHz), SKAO can cover a large area around the LISA detected event down to comparable sensitivity of the reference survey in few tens hour observations, allowing for multiple scans before the final coalescence. Any switched-off source with respect to the reference survey flux will emerge as a strong candidate for the GW source. On the other hand, the unique astrometric precision, resolution and sensitivity of SKA-VLBI will allow to identify the precursor population of massive GW emitters (see above and Sec. 1.2), when the BHs are still spiraling at (sub-)pc scale separations, ultimately covering all the stages of SMBHs mergers.

Finally, as mentioned in Sec. 2, SKAO will offer an unmatched image quality and stable sensitivity in a wide range of angular scales at all observing frequencies. Observing simulations have shown how both SKA-Mid and SKA-Low will dramatically increase the image quality with respect to, e.g., VLBA and LOFAR, even in simple snapshot observations and already with AA* configuration (Braun et al., 2019). The possibility to precisely model the multi-frequency emission of extended and complex sources, from the mas to the degree scales, will revolutionize the field of S-, X- and Z-shaped radio-galaxies and DDRGs (Sec. 1.2). In this respect, the combination of SKA-Mid, SKA-Low and VLBI represent an unique synergy that will allow to distinguish signatures of sub-pc SMBHs pairs, such as the presence of jet precession, by fitting the spectral index maps of these sources with an unprecedented sensitivity and image quality at all physical scales (Rubinur et al., 2017; Kharb et al., 2019).

5 SKAO Science Case 4: Testing simulation predictions

Ahead of the SKAO era, cosmological simulations, which previously could not be compared in detail to observations due to technical limitations, will play a key role in identifying and characterizing AGN populations.

For instance, Thomas et al. (2024) compared the radio excess galaxy population in SIMBA simulation with the MeerKAT international GHz tiered extragalactic exploration (MIGHTEE) survey (Jarvis et al., 2017; Heywood et al., 2022; Whittam et al., 2022), examining their properties as functions of redshift and radio luminosity. They found broad agreement in the overall demographics, such as the similarity in the M_* and $f_{\rm Edd}$ functions for high-excitation and low excitation radio galaxies (HERGs and LERGs, respectively), and confirm the presence of the predicted inefficiently accreting HERG populations. Discrepancies were also uncovered as the HERG–LERG distinction

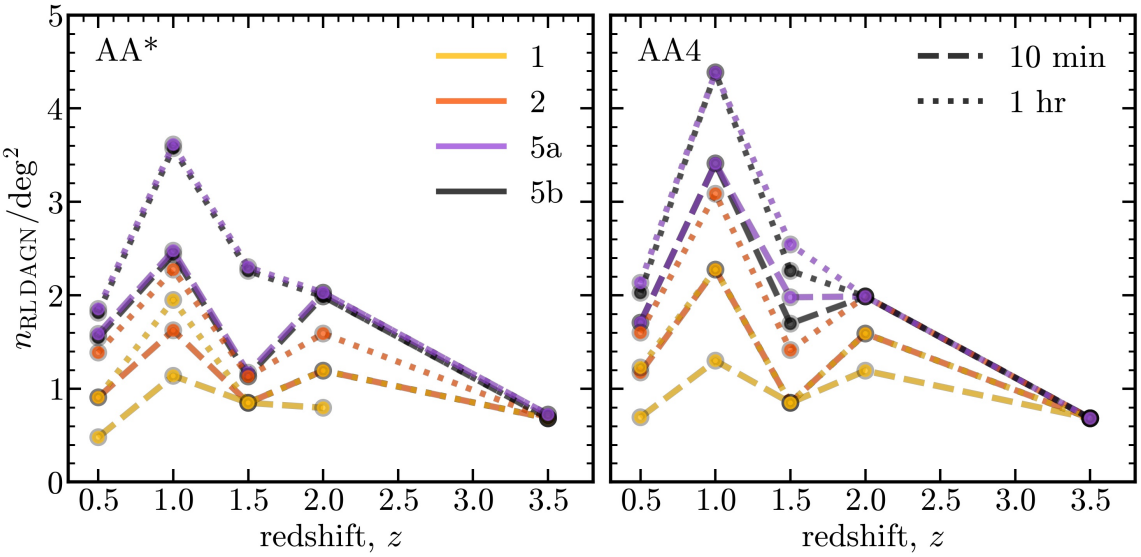

Figure 3: Predicted sky density of RL DAGN per square degree identifiable with SKA AA* (left) and AA4 (right), based on the SIMBA cosmological hydrodynamical simulations. Lines correspond to observation times of 10 minutes (dashed) and 1 hour (dotted) for SKA Bands 1 (yellow), 2 (orange), 5a (purple), and 5b (black). Figure adapted from Pillay et al. (2026).

in SIMBA simulation was found to be more pronounced due to differences in host galaxy gas content. With its superior sensitivity and angular resolution, SKAO will extend such comparisons to the DAGN regime, offering a diverse set of powerful tests of physical models in cosmological simulations.

Furthermore, these simulations provide a framework to forecast the DAGN population potentially observable with the SKAO, as seen in Sec. 3. While Fig. 2 provides a valuable reference to compare current large-scale simulations, Pillay et al. (2026) take a complementary approach, evaluating whether each simulated DAGN would be detectable and spatially resolvable with the projected SKAO capabilities; that is, whether both AGN are bright enough to be detected and sufficiently separated to be resolved.

Following Thomas et al. (2021); Pillay et al. (2026), we adopt the Körding et al. (2008) prescription for the radio emission of SIMBA's DAGN population within 30 pkpc with $M_{\mathrm{BH}} \geq 10^8\,\mathrm{M}_\odot$ and $0 < f_{\mathrm{Edd}} < 0.02$ hosted in galaxies with $M_* \geq 10^{9.5}\,\mathrm{M}_\odot$. The result radio flux density estimates are compared to SKA-Mid sensitivity limits from the current SSC for a hypothetical observation at RA= 0°, Declination = −45°, and a maximum elevation of 59.2° (using resolution-sensitivity balanced visibility weighting corresponding to Briggs robustness = 0).

Figure 3 shows the counts per square degree of RL DAGN predicted to be identifiable with AA4 for a 10-minute and 1-hour observation time; SIMBA predicts up to ∼ 10 RL DAGN per square degree. An SKAO survey of ∼ 7000 deg^2 could thus detect on the order 10^{3-4} RL DAGN, based on these predictions. These results indicate that the all of the simulated systems that are bright enough to be detected are also spatially resolvable. Thus, the effective limit on what can be observed is set by the faintness of the DAGN population and the sensitivity of SKAO (or depth of a given survey).

These results provide a basis for optimizing future SKAO survey strategies by evaluating outcomes across different frequency bands and integration times. This is particularly true when one considers synoptic survey strategies that would reveal both single and dual AGN candidates through flux density variability.

Based on these predictions, the SKA-Mid is well-poised to deliver a statistically significant census of RL DAGN, enabling direct constraints on their abundance, demographics, and evolution.

6 Conclusions and final remarks

In this chapter, we investigated the critical role of the SKAO in achieving a comprehensive understanding of DAGN and SMBHBs. We showed that the study of these multi-SMBH systems is paramount for constraining models of hierarchical galaxy assembly and the co-evolution of SMBHs with their hosts. We highlighted that while radio emission provides a unique, dust-unbiased tool for identifying and confirming multiple accreting SMBHs, current limitations (like insufficient sensitivity and resolution combination, and small area coverage) have hindered the detection of statistically robust samples, particularly for faint, high-z, or obscured sources. SKAO will overcome these constraints through its unmatched combination of sensitivity, angular resolution, image fidelity and survey speed.

We analyzed how SKA-Mid will refine the selection of high-z DAGN candidates previously identified through selection techniques at other wavelengths (mainly optical). Specifically, we detailed how the stable sensitivity and resolution provided by the AA* configuration in Band 5a will enable us to efficiently confirm the DAGN nature of these candidates, exclude contaminants like GLS, and crucially, explore the characteristics of the faint RQ population currently missed by traditional VLBI surveys. Furthermore, we demonstrated that deep reference surveys proposed for SKAO will allow for the blind selection of obscured DAGN. We showed that SKAO will reach the sensitivity necessary (down to nJy/beam levels) to detect systems where both components have bolometric luminosities $L_{\rm bol} > 10^{43}$ erg/s up to $z \sim 2.2$. his capability represents a revolutionary extension beyond current optical limits ($L_{\rm bol} > 10^{45}$ erg/s), promising the detection of potentially hundreds of new DAGN systems during the epoch of cosmic noon.

We investigated the potential for SKAO to trace the entire SMBHBs merger sequence. This includes studying wide-separation pairs in gas-rich mergers like LIRGs and ULIRGs from the local Universe to the cosmic dawn, where radio observation is essential for distinguishing accretion activity from SF. For compact, sub-parsec SMBHBs, we explored indirect signatures, such as jet precession, which generate characteristic large-scale structures like DDRGs and S-, X-, and Z-shaped radio galaxies. Most importantly, we emphasized the critical role of SKA-VLBI in achieving an order-of-magnitude increase in astrometry precision. This will enable us to trace sub-parsec orbital motions via phase referencing (like, e.g., for the binary 3C 66B) and utilize the highly accurate radio-optical centroid offsets—pioneered with SKA-Mid AA* and refined with AA4, to deliver the first statistically robust constraints on binary and recoiling SMBHs in the pc–kpc regime. However, we point out that, despite the unprecedented capabilities of the SKAO, significant interpretative challenges remain, such as those related to the AGN duty cycle. This can prevent the detection

of dual radio cores, where the identification of only a single core in a DAGN can result from a temporarily inactive AGN. At high redshift, in particular, AGN variability can cause the secondary component to be too faint, falling below the sensitivity limit. Nevertheless, we note that in the radio band it may still be possible to detect relic or extended emission (e.g., from older jet activity) even if the core itself is not currently radio-active. High redshift DAGN research can also be affected by foreground contaminants, where the presence of compact radio cores at close projected separation can significantly impact the efficiency of DAGN selection. Disentangling true AGN pairs from projection effects, modeling complex jet structures in low-luminosity or high-redshift environments, and accounting for AGN duty cycles and foreground contamination will require sophisticated modeling and deep multi-wavelength follow-ups to minimize biases.

We established that SKAO is integral to future multi-messenger astrophysics by identifying the electromagnetic counterparts to low-frequency GW events detected by LISA. Its ability to conduct rapid, wide-and-fast monitoring is necessary to pinpoint radio transients, such as temporary jet switch-offs. Finally, we concluded that the demographics and evolution of RL DAGN derived from SKAO observations will provide crucial constraints for cosmological hydrodynamic simulations, moving the field toward observationally driven models of SMBH dynamics and feedback across cosmic time.

References

G. Agazie et al. *ApJL*, 951(1):L9, July 2023. doi: 10.3847/2041-8213/acda9a.

P. Amaro-Seoane et al. *Living Reviews in Relativity*, 26(1):2, Dec. 2023. doi: 10.1007/s41114-022-00041-y.

G. E. Anderson et al. In *Advancing Astrophysics with the SKA – II (AASKAII)*. 2026. arXiv search: Report number AASKAII/GemmaAnderson01.

E. Bañados et al. *ApJ*, 804(2):118, May 2015. doi: 10.1088/0004-637X/804/2/118.

K. Bansal et al. *ApJ*, 843(1):14, July 2017. doi: 10.3847/1538-4357/aa74e1.

M. C. Begelman, R. D. Blandford, and M. J. Rees. *Nature*, 287(5780):307–309, Sept. 1980. doi: 10.1038/287307a0.

S. Bonoli et al. *arXiv e-prints*, art. arXiv:2509.12325, Sept. 2025. doi: 10.48550/arXiv.2509.12325.

M. Bonzini et al. *MNRAS*, 436(4):3759–3771, Dec. 2013. doi: 10.1093/mnras/stt1879.

R. Braun et al. Anticipated performance of the square kilometre array – phase 1 (ska1), 2019. URL https://arxiv.org/abs/1912.12699.

P. Breiding et al. *ApJ*, 914(1):37, June 2021. doi: 10.3847/1538-4357/abfa9a.

N. Chen et al. *MNRAS*, 522(2):1895–1913, June 2023. doi: 10.1093/mnras/stad834.

X. Cheng and B. W. Sohn. *ApJ*, 974(2):155, Oct. 2024. doi: 10.3847/1538-4357/ad6df9.

A. Ciurlo et al. *A&A*, 671:L4, Mar. 2023. doi: 10.1051/0004-6361/202345853.

M. Colpi et al. *arXiv e-prints*, art. arXiv:1903.06867, Mar. 2019. doi: 10.48550/arXiv.1903.06867.

M. Colpi et al. *arXiv e-prints*, art. arXiv:2402.07571, Feb. 2024. doi: 10.48550/arXiv.2402.07571.

J. J. Condon, S. L. O'Dell, J. J. Puschell, and W. A. Stein. *Nature*, 283(5745):357–358, Jan. 1980. doi: 10.1038/283357a0.

J. E. Conway and J. M. Wrobel. *ApJ*, 439:98, Jan. 1995. doi: 10.1086/175155.

Q. D'Amato et al. *A&A*, 668:A133, Dec. 2022. doi: 10.1051/0004-6361/202244452.

A. De Rosa et al. *New Astron. Rev.*, 86:101525, Dec. 2019. doi: 10.1016/j.newar.2020.101525.
R. P. Deane et al. *Nature*, 511(7507):57–60, July 2014. doi: 10.1038/nature13454.
I. Delvecchio et al. *A&A*, 602:A3, June 2017. doi: 10.1051/0004-6361/201629367.
T. Di Matteo, V. Springel, and L. Hernquist. *Nature*, 433(7026):604–607, Feb. 2005. doi: 10.1038/nature03335.
T. Di Matteo, D. Angles-Alcazar, and F. Shankar. *arXiv e-prints*, art. arXiv:2304.11541, Apr. 2023. doi: 10.48550/arXiv.2304.11541.
C. A. Dong-Páez et al. *A&A*, 676:A2, Aug. 2023. doi: 10.1051/0004-6361/202346435.
I. Donnarumma et al. In *Advancing Astrophysics with the Square Kilometre Array (AASKA14)*, page 54, Apr. 2015. doi: 10.22323/1.215.0054.
M. Dotti, M. Colpi, F. Haardt, and L. Mayer. *MNRAS*, 379(3):956–962, Aug. 2007. doi: 10.1111/j.1365-2966.2007.12010.x.
Q. Duan et al. *MNRAS*, 540(1):774–805, June 2025. doi: 10.1093/mnras/staf638.
K. El-Badry, D. W. Hogg, and H.-W. Rix. *arXiv e-prints*, art. arXiv:2509.10601, Sept. 2025. doi: 10.48550/arXiv.2509.10601.
EPTA Collaboration et al. *A&A*, 678:A50, Oct. 2023. doi: 10.1051/0004-6361/202346844.
H. Fu et al. *ApJ*, 745(1):67, Jan. 2012. doi: 10.1088/0004-637X/745/1/67.
Gaia Collaboration et al. *A&A*, 685:A130, May 2024. doi: 10.1051/0004-6361/202347273.
M. Giroletti and F. Panessa. *ApJL*, 706(2):L260–L264, Dec. 2009. doi: 10.1088/0004-637X/706/2/L260.
E. Glikman et al. *ApJL*, 951(1):L18, July 2023. doi: 10.3847/2041-8213/acda2f.
Gopal-Krishna. *A&A*, 688:L16, Aug. 2024. doi: 10.1051/0004-6361/202449409.
M. J. Graham et al. *Nature*, 518(7537):74–76, Feb. 2015. doi: 10.1038/nature14143.
A. C. Gross et al. *ApJ*, 883(1):50, Sept. 2019. doi: 10.3847/1538-4357/ab3795.
K. Gültekin et al. *ApJ*, 706(1):404–416, Nov. 2009. doi: 10.1088/0004-637X/706/1/404.
M. Habouzit et al. *MNRAS*, 509(2):3015–3042, Jan. 2022. doi: 10.1093/mnras/stab3147.
C. L. Hale et al. *MNRAS*, 536(3):2187–2211, Jan. 2025. doi: 10.1093/mnras/stae2528.
I. Heywood et al. *MNRAS*, 509(2):2150–2168, Jan. 2022. doi: 10.1093/mnras/stab3021.
A. P. S. Hygate et al. *MNRAS*, 524(2):1775–1795, Sept. 2023. doi: 10.1093/mnras/stad1212.
Ž. Ivezić et al. *ApJ*, 873(2):111, Mar. 2019. doi: 10.3847/1538-4357/ab042c.
K. Iwasawa et al. *A&A*, 529:A106, May 2011. doi: 10.1051/0004-6361/201015264.
A. H. Jaffe and D. C. Backer. *ApJ*, 583(2):616–631, Feb. 2003. doi: 10.1086/345443.
M. J. Jarvis et al. The meerkat international ghz tiered extragalactic exploration (mightee) survey, 2017. URL https://arxiv.org/abs/1709.01901.
F. A. Jenet, A. Lommen, S. L. Larson, and L. Wen. In F. A. Rasio and I. H. Stairs, editors, *Binary Radio Pulsars*, volume 328 of *Astronomical Society of the Pacific Conference Series*, page 399, July 2005.
J. I. Katz. *ApJ*, 478(2):527–529, Mar. 1997. doi: 10.1086/303811.
P. Kharb, D. V. Lal, and D. Merritt. *Nature Astronomy*, 1:727–733, Sept. 2017. doi: 10.1038/s41550-017-0256-4.
P. Kharb et al. *ApJ*, 871(2):249, Feb. 2019. doi: 10.3847/1538-4357/aafad7.
P. Kharb et al. *ApJ*, 919(2):108, Oct. 2021. doi: 10.3847/1538-4357/ac0c82.
H. Kobayashi et al. In *Advancing Astrophysics with the SKA – II (AASKAII)*. 2026. arXiv search:

Report number AASKAII/Kobayashi01.

W. Kollatschny et al. *A&A*, 633:A79, Jan. 2020. doi: 10.1051/0004-6361/201936540.

S. Komossa and D. Grupe. *Serbian Astronomical Journal*, 209:1–24, Dec. 2024. doi: 10.2298/SAJ2409001K.

S. Komossa et al. *ApJL*, 582(1):L15–L19, Jan. 2003. doi: 10.1086/346145.

S. Komossa et al. *MNRAS*, 522(1):L84–L88, June 2023a. doi: 10.1093/mnrasl/slad016.

S. Komossa et al. *ApJ*, 944(2):177, Feb. 2023b. doi: 10.3847/1538-4357/acaf71.

E. G. Körding, S. Jester, and R. Fender. *MNRAS*, 383(1):277–288, Jan. 2008. doi: 10.1111/j.1365-2966.2007.12529.x.

J. Kormendy and L. C. Ho. *ARA&A*, 51(1):511–653, Aug. 2013. doi: 10.1146/annurev-astro-082708-101811.

J. Kormendy and D. Richstone. *ARA&A*, 33:581, Jan. 1995. doi: 10.1146/annurev.aa.33.090195.003053.

M. J. Koss et al. *ApJL*, 942(1):L24, Jan. 2023. doi: 10.3847/2041-8213/aca8f0.

Y. Li et al. *Research in Astronomy and Astrophysics*, 24(7):072001, July 2024. doi: 10.1088/1674-4527/ad420c.

F. K. Liu and X. Chen. *ApJ*, 671(2):1272–1283, Dec. 2007. doi: 10.1086/522910.

F. K. Liu, S. Li, and S. Komossa. *ApJ*, 786(2):103, May 2014. doi: 10.1088/0004-637X/786/2/103.

A. P. Lobanov. *A&A*, 330:79–89, Feb. 1998. doi: 10.48550/arXiv.astro-ph/9712132.

V. V. Makarov et al. *ApJL*, 835(2):L30, Feb. 2017. doi: 10.3847/2041-8213/835/2/L30.

A. Mangiagli et al. *Phys. Rev. D*, 102(8):084056, Oct. 2020. doi: 10.1103/PhysRevD.102.084056.

F. Mannucci et al. *Nature Astronomy*, 6:1185–1192, Aug. 2022. doi: 10.1038/s41550-022-01761-5.

F. Mannucci et al. *A&A*, 680:A53, Dec. 2023. doi: 10.1051/0004-6361/202346894.

A. P. Marscher et al. *Nature*, 452(7190):966–969, Apr. 2008. doi: 10.1038/nature06895.

Y. Matsuoka et al. *ApJL*, 965(1):L4, Apr. 2024. doi: 10.3847/2041-8213/ad35c7.

L. Mayer et al. *Science*, 316(5833):1874, June 2007. doi: 10.1126/science.1141858.

D. L. Meier. *ApJL*, 548(1):L9–L12, Feb. 2001. doi: 10.1086/318921.

A. Merloni, S. Heinz, and T. di Matteo. *MNRAS*, 345(4):1057–1076, Nov. 2003. doi: 10.1046/j.1365-2966.2003.07017.x.

D. Merritt. *Dynamics and Evolution of Galactic Nuclei*. 2013.

M. Milosavljević and E. S. Phinney. *ApJL*, 622(2):L93–L96, Apr. 2005. doi: 10.1086/429618.

C. M. F. Mingarelli et al. *Nature Astronomy*, 9:183–184, Feb. 2025. doi: 10.1038/s41550-025-02482-1.

A. Misra, M. Jamrozy, M. Weżgowiec, and D. Kozieł-Wierzbowska. *MNRAS*, 536(3):2025–2045, Jan. 2025. doi: 10.1093/mnras/stae2639.

L. K. Morabito et al. *MNRAS*, 515(4):5758–5774, Oct. 2022. doi: 10.1093/mnras/stac2129.

S. Nandi et al. *MNRAS*, 467(1):L56–L60, May 2017. doi: 10.1093/mnrasl/slw256.

S. Nandi et al. *ApJ*, 965(1):9, Apr. 2024. doi: 10.3847/1538-4357/ad2c92.

S. O'Neill et al. *ApJL*, 926(2):L35, Feb. 2022. doi: 10.3847/2041-8213/ac504b.

F. Panessa and M. Giroletti. *MNRAS*, 432(2):1138–1143, June 2013. doi: 10.1093/mnras/stt547.

F. Panessa et al. *MNRAS*, 447(2):1289–1298, Feb. 2015. doi: 10.1093/mnras/stu2455.

Z. Paragi et al. In *Advancing Astrophysics with the Square Kilometre Array (AASKA14)*, page 143, Apr. 2015. doi: 10.22323/1.215.0143.

M. Perna et al. *A&A*, 696:A59, Apr. 2025. doi: 10.1051/0004-6361/202453430.

L. Petrov, Y. Y. Kovalev, and A. V. Plavin. *MNRAS*, 482(3):3023–3031, Jan. 2019. doi: 10.1093/mnras/sty2807.

C. Pillay, R. Deane, and R. Davé. Simba predictions of dual active galactic nuclei in future meerkat+ and ska-mid surveys. in preparation, 2026.

A. V. Plavin, Y. Y. Kovalev, and L. Y. Petrov. *ApJ*, 871(2):143, Feb. 2019. doi: 10.3847/1538-4357/aaf650.

I. Prandoni and N. Seymour. In *Advancing Astrophysics with the Square Kilometre Array (AASKA14)*, page 67, Apr. 2015. doi: 10.22323/1.215.0067.

C. Puerto-Sánchez et al. *MNRAS*, 536(3):3016–3040, Jan. 2025. doi: 10.1093/mnras/stae2763.

C. Rodriguez et al. *ApJ*, 646(1):49–60, July 2006. doi: 10.1086/504825.

K. Rubinur, M. Das, P. Kharb, and M. Honey. *MNRAS*, 465(4):4772–4782, Mar. 2017. doi: 10.1093/mnras/stw2981.

K. Rubinur, M. Das, and P. Kharb. *MNRAS*, 484(4):4933–4950, Apr. 2019. doi: 10.1093/mnras/stz334.

D. B. Sanders and I. F. Mirabel. *ARA&A*, 34:749, Jan. 1996. doi: 10.1146/annurev.astro.34.1.749.

E. Schwartzman et al. *ApJ*, 987(2):200, July 2025. doi: 10.3847/1538-4357/add47c.

M. Scialpi et al. *A&A*, 690:A57, Oct. 2024. doi: 10.1051/0004-6361/202347242.

A. Sesana. *MNRAS*, 433:L1–L5, June 2013. doi: 10.1093/mnrasl/slt034.

A. Sesana. *Frontiers in Astronomy and Space Sciences*, 8:7, Feb. 2021. doi: 10.3389/fspas.2021.601646.

R. M. Shannon et al. In *Advancing Astrophysics with the SKA – II (AASKAII)*. 2026. arXiv search: Report number AASKAII/Shannon01.

X. Shen et al. *MNRAS*, 495(3):3252–3275, Jan. 2020. doi: 10.1093/mnras/staa1381.

Y. Shen, H.-C. Hwang, N. Zakamska, and X. Liu. *ApJL*, 885(1):L4, Nov. 2019. doi: 10.3847/2041-8213/ab4b54.

Y. Shen et al. *ApJ*, 943(1):38, Jan. 2023. doi: 10.3847/1538-4357/aca662.

T. W. Shimwell et al. *A&A*, 598:A104, Feb. 2017. doi: 10.1051/0004-6361/201629313.

X. Shu et al. In *Advancing Astrophysics with the SKA – II (AASKAII)*. 2026. arXiv search: Report number AASKAII/Shu01.

A. Sillanpaa et al. *ApJ*, 325:628, Feb. 1988. doi: 10.1086/166033.

C. J. Skipper and I. W. A. Browne. *MNRAS*, 475(4):5179–5193, Apr. 2018. doi: 10.1093/mnras/sty114.

V. Smolčić et al. *A&A*, 602:A2, June 2017. doi: 10.1051/0004-6361/201630223.

C. Spingola, J. P. McKean, D. Massari, and L. V. E. Koopmans. *A&A*, 630:A108, Oct. 2019. doi: 10.1051/0004-6361/201935427.

C. Spingola et al. *A&A*, 643:L12, Nov. 2020. doi: 10.1051/0004-6361/202039458.

C. Spingola et al. In *Advancing Astrophysics with the SKA – II (AASKAII)*. 2026. arXiv search: Report number AASKAII/Spingola01.

H. Sudou, S. Iguchi, Y. Murata, and Y. Taniguchi. *Science*, 300(5623):1263–1265, May 2003. doi: 10.1126/science.1082817.

K. Takahashi et al. In *Advancing Astrophysics with the SKA – II (AASKAII)*. 2026. arXiv search: Report number AASKAII/Takahashi01.

S. Tang et al. *MNRAS*, 538(4):3001–3022, Apr. 2025. doi: 10.1093/mnras/staf416.

Y. Terashima and A. S. Wilson. *ApJ*, 583(1):145–158, Jan. 2003. doi: 10.1086/345339.

N. Thomas, R. Davé, M. J. Jarvis, and D. Anglés-Alcázar. *MNRAS*, 503(3):3492–3509, 2021. doi: 10.1093/mnras/stab654.

N. L. Thomas et al. *Monthly Notices of the Royal Astronomical Society*, 536(3):2873–2890, Dec. 2024. ISSN 1365-2966. doi: 10.1093/mnras/stae2724. URL http://dx.doi.org/10.1093/mnras/stae2724.

A. Toubiana et al. *arXiv e-prints*, art. arXiv:2410.17916, Oct. 2024. doi: 10.48550/arXiv.2410.17916.

M. Tremmel et al. *MNRAS*, 470(1):1121–1139, Sept. 2017. doi: 10.1093/mnras/stx1160.

A. Trindade Falcão et al. *ApJ*, 972(2):185, Sept. 2024. doi: 10.3847/1538-4357/ad6b91.

A. Tripathi et al. *ApJ*, 977(2):166, Dec. 2024. doi: 10.3847/1538-4357/ad90e3.

H. Übler et al. *MNRAS*, 531(1):355–365, June 2024. doi: 10.1093/mnras/stae943.

E. Valtaoja et al. *ApJ*, 531(2):744–755, Mar. 2000. doi: 10.1086/308494.

M. J. Valtonen et al. *Nature*, 452(7189):851–853, Apr. 2008. doi: 10.1038/nature06896.

S. Vaughan et al. *MNRAS*, 461(3):3145–3152, Sept. 2016. doi: 10.1093/mnras/stw1412.

M. Villata, C. M. Raiteri, A. Sillanpaa, and L. O. Takalo. *MNRAS*, 293(1):L13–L16, Jan. 1998. doi: 10.1046/j.1365-8711.1998.01244.x.

M. Volonteri, P. Madau, and F. Haardt. *ApJ*, 593(2):661–666, Aug. 2003. doi: 10.1086/376722.

M. Volonteri et al. *MNRAS*, 514(1):640–656, July 2022. doi: 10.1093/mnras/stac1217.

I. H. Whittam et al. *Monthly Notices of the Royal Astronomical Society*, 516(1):245–263, Aug. 2022. ISSN 1365-2966. doi: 10.1093/mnras/stac2140. URL http://dx.doi.org/10.1093/mnras/stac2140.

W. Xu et al. *ApJ*, 969(1):36, July 2024. doi: 10.3847/1538-4357/ad463b.

M. Yue, X. Fan, J. Yang, and F. Wang. *ApJL*, 921(2):L27, Nov. 2021. doi: 10.3847/2041-8213/ac31a9.

M. Yue, X. Fan, J. Yang, and F. Wang. *AJ*, 165(5):191, May 2023. doi: 10.3847/1538-3881/acc2be.